SCIENCE CHINA
Earth Sciences

• RESEARCH PAPER •

March 2014 Vol.57 No.3: 542–549
doi: 10.1007/s11430-013-4783-2

Seismic wave scattering inversion for fluid factor of heterogeneous media

YIN XingYao*, ZONG ZhaoYun & WU GuoChen

School of Geosciences, China University of Petroleum (Huadong), Qingdao 266580, China

Received January 4, 2013; accepted May 24, 2013; published online December 24, 2013

Elastic wave inverse scattering theory plays an important role in parameters estimation of heterogeneous media. Combining inverse scattering theory, perturbation theory and stationary phase approximation, we derive the P-wave seismic scattering coefficient equation in terms of fluid factor, shear modulus and density of background homogeneous media and perturbation media. With this equation as forward solver, a pre-stack seismic Bayesian inversion method is proposed to estimate the fluid factor of heterogeneous media. In this method, Cauchy distribution is utilized to the ratios of fluid factors, shear moduli and densities of perturbation media and background homogeneous media, respectively. Gaussian distribution is utilized to the likelihood function. The introduction of constraints from initial smooth models enhances the stability of the estimation of model parameters. Model test and real data example demonstrate that the proposed method is able to estimate the fluid factor of heterogeneous media from pre-stack seismic data directly and reasonably.

heterogeneous media, fluid factor, seismic wave scattering, pre-stack seismic inversion

Citation: Yin X Y, Zong Z Y, Wu G C. 2014. Seismic wave scattering inversion for fluid factor of heterogeneous media. Science China: Earth Sciences, 57: 542–549, doi: 10.1007/s11430-013-4783-2

Amplitude variation with offset (AVO) inversion and acoustic/elastic inverse scattering inversion have been much studied in seismic exploration and development. The former has been widely applied in lithology prediction and the latter is beneficial to fluid discrimination. In seismic exploration, pre-stack seismic data contain abundant information related to elastic and reservoir parameters. The exact or approximate Zoeppritz equations (Zoeppritz et al., 1919; Liu et al., 2010; Yang et al., 2008; Chen et al., 2007) describe the seismic wave reflection/transmission coefficients in terms of elastic parameters in upper and lower media under the horizontal layered hypothesis. The parameters underground can be estimated in most conditions (Buland et al., 2003; Smith et al., 1987; Zong et al., 2012a, 2012b) with the Exact or approximate Zoeppritz equations. However, when the heterogeneous targets including fractures or caves exist, seismic wave scattering occurs (Burns et al., 2007; Kaslilar, 2007; Scarpetta et al., 2008). In theory, the seismic reflection coefficients with horizontal layered hypothesis do not work in this condition.

Acoustic and elastic wave inverse scattering inversion plays an important role in parameters estimation of heterogeneous media (Weglein, 1993; Zhang et al., 2009a, 2009b). Born or Rytov approximations (Mora et al., 1987; Rajan et al., 1989; Stolt et al., 1985) have been widely utilized in seismic image or inversion. With the perturbation theory, the heterogeneous media can be seen as the superposition of background media and perturbation media. Miles (1960) derived Rayleigh scattering equation with the Born approximation based on volume integral equation. Hudson (1968, 1977) derived the scattering equation of conventional weak heterogeneous media in a similar approach. Wu et al. (1985) described the Rayleigh scattering with different

*Corresponding author (email: xyyin@upc.edu.cn)

point and moment force and studied the scattering characteristics in different conditions. Beylkin et al. (1990) found that the scattering function was related to the scattering coefficients and the scale factor of incident angle. Liu et al. (2000, 2001) studied the simulation of multiple scattering of seismic waves by spatially distributed inclusions and effects of multiple fracture sets on shear-wave polarizations in fluid discrimination (Liu et al., 2001). Shaw (2004) studied the scattering characteristics of anisotropic media. Boit (1956, 1962) and Gassmann (1951) theories have been widely applied in fluid discrimination with pre-stack seismic data. Zong et al. (2012b) reestablished the relationship between fluid factor and P-wave and S-wave moduli with Biot Gassmann theory. Seismic wave scattering theory has been studied extensively in seismic wave modeling, image, and attenuation, but its application to fluid discrimination of heterogeneous media has not been adequately studied. In this paper, with the stationary phase method in the first order approximation of elastic wave scattering, the seismic wave scattering coefficient of heterogeneous media is derived in terms of fluid factor, shear modulus and density. With this equation as forward solver, a pre-stack seismic Bayesian inversion method is proposed to estimate the fluid factor of the heterogeneous media.

1 P-wave scattering coefficient in terms of fluid factor, shear modulus and density of heterogeneous media

Under weak scattering hypothesis, the elastic scattered wave $\boldsymbol{u}^s$ can be expressed as (Cervený, 2000),

$$\boldsymbol{u}^s\left(\boldsymbol{x}',\omega\right)=\int_V\left(\omega^2\Delta\rho\left(\boldsymbol{x}^s\right)u_i^0\left(\boldsymbol{x}^s,\omega\right)G_{mi}^0\left(\boldsymbol{x}^s,\omega;\boldsymbol{x}'\right)\right.$$
$$\left.-\Delta c_{ijkl}\left(\boldsymbol{x}'\right)\frac{\partial u_k^0\left(\boldsymbol{x}^s,\omega\right)}{\partial x_l}\frac{\partial G_{mi}^0\left(\boldsymbol{x}^s,\omega;\boldsymbol{x}'\right)}{\partial x_j}\right)\mathrm{d}\boldsymbol{x}^s, \quad (1)$$

where $\boldsymbol{u}^s$ is the elastic wave field simulated by $\boldsymbol{x}^s$ at point $\boldsymbol{x}'$. u^0 is the elastic wave field of homogeneous media. ω is the circular frequency. $u_i^0(\bullet)$ and $G_{mi}^0(\bullet)$ are the elastic wave field of source and Green function, respectively. $G_{mi}^0\left(\boldsymbol{x}^s,\omega;\boldsymbol{x}'\right)$ is the displacement of source $\boldsymbol{x}^s$ at receiver $\boldsymbol{x}'$. $\Delta\rho=\rho-\rho_0$, ρ and ρ_0 are densities of homogeneous and perturbation media, respectively.

$$\Delta c_{ijkl}=\begin{bmatrix}\Delta M & \Delta M-2\Delta\mu & \Delta M-2\Delta\mu & 0 & 0 & 0\\ \Delta M-2\Delta\mu & \Delta M & \Delta M-2\Delta\mu & 0 & 0 & 0\\ \Delta M-2\Delta\mu & \Delta M-2\Delta\mu & \Delta M & 0 & 0 & 0\\ 0 & 0 & 0 & \Delta\mu & 0 & 0\\ 0 & 0 & 0 & 0 & \Delta\mu & 0\\ 0 & 0 & 0 & 0 & 0 & \Delta\mu\end{bmatrix}.$$

ΔM and $\Delta\mu$ are P-wave and S-wave moduli of perturbation media, respectively. Supposing the elastic wave field $u_{mi}\left(\boldsymbol{x}',\omega\right)$ at $\boldsymbol{x}'$ is from $\boldsymbol{x}^s$,

$$u_{mi}\left(\boldsymbol{x}',\omega\right)=G_{mi}\left(\boldsymbol{x}^s,\omega;\boldsymbol{x}'\right). \quad (2)$$

If the harmonic function of the point source is expressed as

$$\boldsymbol{G}\left(\boldsymbol{r},\omega\right)=\frac{N_nN_i}{4\pi\rho_0\alpha_0^2}\frac{1}{\boldsymbol{r}}\mathrm{e}^{i\omega\boldsymbol{r}/\alpha_0}, \quad (3)$$

where N_n and N_i are the directions of the point source and receiver, respectively. α_0 is the P-wave velocity of background homogeneous media. $\boldsymbol{r}$ is the distance from source to receiver. Substituting eq. (2) and (3) into eq. (1) yields

$$\boldsymbol{u}^s\left(\boldsymbol{r},\omega\right)=N_mM_n\omega^2$$
$$\times\int_V\mathrm{d}\boldsymbol{r}\left[\left(\Delta\rho\delta_{ik}+\Delta c_{ijkl}s_j^ss_l\right)p_i^sp_k\right]A\left(\boldsymbol{r}\right)\mathrm{e}^{i\omega\varphi(\boldsymbol{r})}, \quad (4)$$

where $\boldsymbol{s}$ and $\boldsymbol{s}^s$ are the slowness vectors of incident wave and scattering wave, respectively. $\boldsymbol{p}$ and $\boldsymbol{p}^s$ are the polarization vectors of incident wave and scattering wave, respectively. N_m is the projection of the source direction into the incident ray. M_n is the projection of the receiver direction into the scattering ray. N_mM_n denotes the couple of the source and receiver. $\varphi(\boldsymbol{r})$ denotes the phase after scattering, and $A(\boldsymbol{r})$ is the amplitude,

$$A\left(\boldsymbol{r}\right)=\frac{1}{\left(4\pi\rho_0\alpha_0^2\right)^2}\frac{1}{\boldsymbol{r}^2}. \quad (5)$$

From eqs. (4) and (5), we can see that the amplitude of scattering wave varies slowly. However, the phase varies fast. Therefore, we can solve eq. (4) with the stationary phase approximation (Shaw et al., 2004). The P-wave scattering wave field at $\boldsymbol{r}=\boldsymbol{r}_0$ can be expressed as

$$\boldsymbol{u}^s\left(\boldsymbol{r},\omega\right)=-N_mM_n\frac{1}{4\pi\rho_0\alpha_0^2\boldsymbol{r}_0}$$
$$\times\left(\frac{1}{4\rho_0\cos^2\theta}\left(\Delta\rho\delta_{ik}+\Delta c_{ijkl}s_j^ss_l\right)p_i^sp_k\big|_{r=r_0}\right)\mathrm{e}^{i\omega\varphi(\boldsymbol{r}_0)}. \quad (6)$$

Combining eq. (3) and eq. (6) yields

$$\boldsymbol{u}^s\left(\boldsymbol{r},\omega\right)=-\frac{N_mM_n}{4\pi\rho_0\alpha_0^2\boldsymbol{r}_0}\mathrm{e}^{i\omega\varphi(\boldsymbol{r}_0)}R\left(\theta\right)=-G_{mn}\left(\boldsymbol{r},\omega\right)R\left(\theta\right), \quad (7)$$

where $R(\theta)$ can be defined as the P-wave scattering coefficient at incident θ,

$$R(\theta)=\frac{1}{4M_0\cos^2\theta}\Delta M-\frac{2\sin^2\theta}{M_0}\Delta\mu+\frac{1}{2\rho_0}\left(1-\frac{1}{2\cos^2\theta}\right)\Delta\rho. \quad (8)$$

Zong et al. (2012b) reestablished the fluid factor in terms of P-wave and S-wave moduli as

$$f_0=M_0-k_{dry}\mu_0, \quad (9)$$

where f_0 is the fluid factor of background homogeneous media. M_0 and μ_0 are P-wave modulus and S-wave modulus, respectively. k_{dry} is the ratio of P-wave velocity and S-wave velocity of dry rock (Russell et al., 2003).

Taking differential of both sides of equation (9) yields

$$\Delta M_0=\Delta f_0+k_{dry}\Delta\mu_0, \quad (10)$$

and

$$\frac{1}{M_0}=\frac{1}{k_{sat}\mu_0}=\left(1-\frac{k_{dry}}{k_{sat}}\right)\times\frac{1}{f_0}. \quad (11)$$

Substituting eqs. (10) and (11) into eq. (8) yields

$$R(\theta)=a(\theta)\Delta f+b(\theta)\Delta\mu+c(\theta)\Delta\rho, \quad (12)$$

where

$$a(\theta)=\frac{\sec^2\theta}{4f_0}\left(1-\frac{k_{dry}}{k_{sat}}\right),$$
$$b(\theta)=\frac{\left(k_{dry}\sec^2\theta-8\sin^2\theta\right)}{4k_{sat}\mu_0},$$
$$c(\theta)=\frac{1}{2\rho_0}\left(1-\frac{\sec^2\theta}{2}\right),$$

where k_{sat} is the ratio of saturated rock. This equation establishes the relationship between P-wave scattering coefficient and fluid factors, shear moduli and densities of background homogeneous media and perturbation media.

2 Bayesian inversion for fluid factor

With eq. (12), in Bayesian inversion scheme, Cauchy distribution is utilized to the ratios of fluid factor, shear modulus and density of perturbation media and background homogeneous media. Gaussian distribution is utilized to the likelihood function. With Bayesian theory, the post probability function can be obtained. The introduction of initial smooth model and multi-iteration enhances the stability of the inversion.

Rearranging eq. (12) yields

$$R(\theta)=A(\theta)\frac{\Delta f}{f_0}+B(\theta)\frac{\Delta\mu}{\mu_0}+C(\theta)\frac{\Delta\rho}{\rho_0}. \quad (13)$$

Defining $L_f=\frac{\Delta f}{f_0}$, $L_\mu=\frac{\Delta\mu}{\mu_0}$, $L_\rho=\frac{\Delta\rho}{\rho_0}$, eq. (12) becomes

$$R(\theta)=A(\theta)L_f+B(\theta)L_\mu+C(\theta)L_\rho. \quad (14)$$

If there are N offsets, M samples, eq. (14) can be expressed in matrix form as,

$$\begin{bmatrix}\bar{R}_1\\ \bar{R}_2\\ \vdots\\ \bar{R}_M\end{bmatrix}=\begin{bmatrix}\bar{A}_1 & \bar{B}_1 & \bar{C}_1\\ \bar{A}_2 & \bar{B}_2 & \bar{C}_2\\ & \cdots & \\ \bar{A}_M & \bar{B}_M & \bar{C}_M\end{bmatrix}\begin{bmatrix}\bar{L}_f\\ \bar{L}_\mu\\ \bar{L}_\rho\end{bmatrix}, \quad (15)$$

where $\bar{R}_1=\left[R_1^1 \ \ldots \ R_1^N\right]^{\mathrm{T}}$, $\bar{A}_1=diag\left[A_1^1 \ \ldots \ A_1^N\right]$, $\bar{L}_f=\left[L_f^1 \ \ldots \ L_f^N\right]^{\mathrm{T}}$. T denotes the transform of matrix, and so on. Considering the effluence of wavelet (Downton et al., 2004), eq. (15) can be expressed as

$$\boldsymbol{D}_{NM\times1}=\boldsymbol{G}_{NM\times3N}\cdot\boldsymbol{L}_{3N\times1}, \quad (16)$$

where $\boldsymbol{G}$ is the forward solver matrix. $\boldsymbol{L}$ is the parameters to be estimated.

Cauchy distribution (Downton et al., 2004) is utilized to the parameters to be estimated and Gaussian distribution (Buland et al., 2003) is utilized to the likelihood function. We yield the post probability distribution function as

$$p(\boldsymbol{L},\sigma_n\mid\boldsymbol{D})\propto\prod_{i=1}^{M}\left[\frac{1}{1+\boldsymbol{L}_i^2/\sigma_m^2}\right]\times\exp\left[-\frac{(\boldsymbol{D}-\boldsymbol{GL})^{\mathrm{T}}(\boldsymbol{D}-\boldsymbol{GL})}{2\sigma_n^2}\right], \quad (17)$$

where $\boldsymbol{D}$ is the pre-stack seismic data, $\sigma_n{}^2$ is the variance of noise, σ_m^2 is the variance of parameters to be estimated, M is the number of model parameters, n is the number of samples, and $\boldsymbol{L}_i$ is the ith parameter to be estimated.

Maximizing eq. (17) yields

$$F(\boldsymbol{L})=(\boldsymbol{D}-\boldsymbol{GL})^{\mathrm{T}}(\boldsymbol{D}-\boldsymbol{GL})+2\sigma_n{}^2\sum_{i=1}^{M}\ln(1+\boldsymbol{L}_i^2/\sigma_m^2). \quad (18)$$

Adding the constraint from initial smooth model and minimizing the kernel function yields

$$\begin{aligned}&(\boldsymbol{G}^{\mathrm{T}}\boldsymbol{G}+\lambda_c\boldsymbol{Q}+\lambda_f\boldsymbol{P}_f^T\boldsymbol{P}_f+\lambda_\mu\boldsymbol{P}_\mu^T\boldsymbol{P}_\mu+\lambda_\rho\boldsymbol{P}_\rho^T\boldsymbol{P}_\rho)\boldsymbol{L}\\&=(\boldsymbol{G}^{\mathrm{T}}\boldsymbol{D}+\boldsymbol{P}_f^T\boldsymbol{\eta}_f+\boldsymbol{P}_\mu^T\boldsymbol{\eta}_\mu+\boldsymbol{P}_\rho^T\boldsymbol{\eta}_\rho),\end{aligned} \quad (19)$$

where $\lambda_i, i=f,\mu,\rho$ are constraint coefficients of fluid factor, shear modulus and density. λ_c is the constraint coefficient of Cauchy prior information, $\lambda_c=2\sigma_n{}^2/\sigma_m^2$, $Q=diag\left[\frac{1}{(1+L_1{}^2/\sigma_m^2)^2},\frac{1}{(1+L_2{}^2/\sigma_m^2)^2},\ldots,\frac{1}{(1+L_M{}^2/\sigma_m^2)^2}\right]$.

$\boldsymbol{P}_i, i = f, \mu, \rho$ denotes the constraint matrix of model, $\boldsymbol{\eta}_i = (\boldsymbol{L}_0)_i, i = f, \mu, \rho$. $\boldsymbol{L}_0$ is the initial smooth model of parameters to be estimated.

Eq. (19) can be expressed as

$$\boldsymbol{\Psi} = \boldsymbol{KL}, \tag{20}$$

where

$$\boldsymbol{\Psi} = \boldsymbol{G}^{\mathrm{T}}\boldsymbol{D} + \boldsymbol{P}_f^T\boldsymbol{\eta}_f + \boldsymbol{P}_\mu^T\boldsymbol{\eta}_\mu + \boldsymbol{P}_\rho^T\boldsymbol{\eta}_\rho,$$

$$\boldsymbol{K} = \boldsymbol{G}^{\mathrm{T}}\boldsymbol{G} + \lambda_c\boldsymbol{Q} + \lambda_f\boldsymbol{P}_f^T\boldsymbol{P}_f + \lambda_\mu\boldsymbol{P}_\mu^T\boldsymbol{P}_\mu + \lambda_\rho\boldsymbol{P}_\rho^T\boldsymbol{P}_\rho.$$

Singular value decomposition (SVD) is one of the efficient ways to solve inverse problem. Applying SVD to $\boldsymbol{K}$ yields

$$\boldsymbol{K} = \boldsymbol{U\Lambda V}^{\mathrm{T}}, \tag{21}$$

where $\boldsymbol{\Lambda}$ is the diagonal matrix,

$$\boldsymbol{\Lambda} = \begin{bmatrix} \sigma_1 & 0 & \cdots & 0 \\ 0 & \sigma_2 & \cdots & 0 \\ \cdots & \cdots & \cdots & \cdots \\ 0 & 0 & \cdots & \sigma_{3N} \end{bmatrix}_{3N\times 3N}. \tag{22}$$

The generalized inverse of $\boldsymbol{K}$ is,

$$\boldsymbol{K}_g^+ = \boldsymbol{V\Lambda}^{-1}\boldsymbol{U}^{\mathrm{T}} = \boldsymbol{V}\left[diag\left(\frac{1}{\sigma_{3N}}\right)\right]\boldsymbol{U}^{\mathrm{T}}. \tag{23}$$

Combining eqs. (20) and (23) yields

$$\boldsymbol{L}^{est} = \boldsymbol{V\Lambda}^{-1}\boldsymbol{U}^T\boldsymbol{\Psi}, \tag{24}$$

where $\boldsymbol{L}^{est}$ is the estimated value of the model parameter.

With eq. (24), we can obtain the first iteration result of L_{f1}, $L_{\mu 1}$ and $L_{\rho 1}$. Taking the fluid factor for example, the first iteration result of fluid factor is

$$f_1 = L_{f1}f_0 + f_0 = f_0\left(1 + L_{f1}\right), \tag{25}$$

where f_0 is the fluid factor of background homogeneous media. After t iterations, the fluid factor f_t of heterogeneous media can be yielded as

$$f_t = f_0\prod_{i=1}^{t}\left(1 + L_{fi}\right)^i. \tag{26}$$

Similarly,

$$\mu_t = \mu_0\prod_{i=1}^{t}\left(1 + L_{\mu i}\right)^i, \tag{27}$$

$$\rho_t = \rho_0\prod_{i=1}^{t}\left(1 + L_{\rho i}\right)^i. \tag{28}$$

3 Model test

Real well curves model is utilized to verify the feasibility and stability of the inversion approach proposed in this paper. The blue curves in Figure 1 are the fluid factor, shear

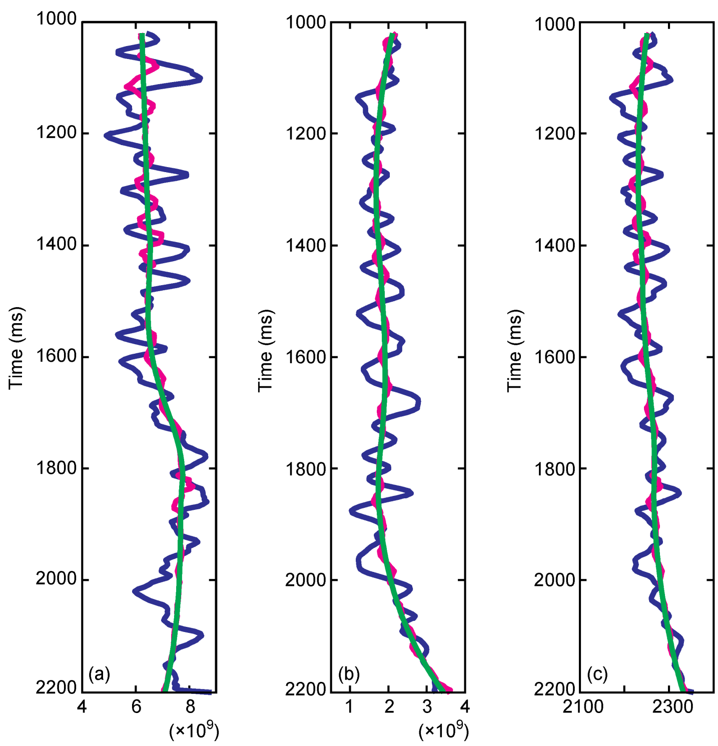

Figure 1 Model curves (blue), initial models (green) and the inversion results (pink) after first iteration without noise. (a) Fluid factor (N/m^2); (b) shear modulus (N/m^2); (c) density (kg/m^3).

modulus and density of the known well in time domain, respectively. With seismic wavelet whose main frequency is about 40 Hz, the pre-stack angle gather can be simulated as observed data. The green curves in Figure 1 are the initial smooth models of the fluid factor, shear modulus and density of the known well, respectively, and the pink ones are the inversion results after the first iteration. Figure 2 displays the inversion results of the fluid factor, shear modulus and density after 5 iterations, respectively. From Figures 1 and 2, we demonstrate that the fluid factor, shear modulus and density can be reasonably estimated after 5 iterations with 1.1% error. Figures 3 and 4 display the inversion results of the fluid factor, shear modulus and density under the condition with S/N ratio 5:1 and 2:1 of observed data,

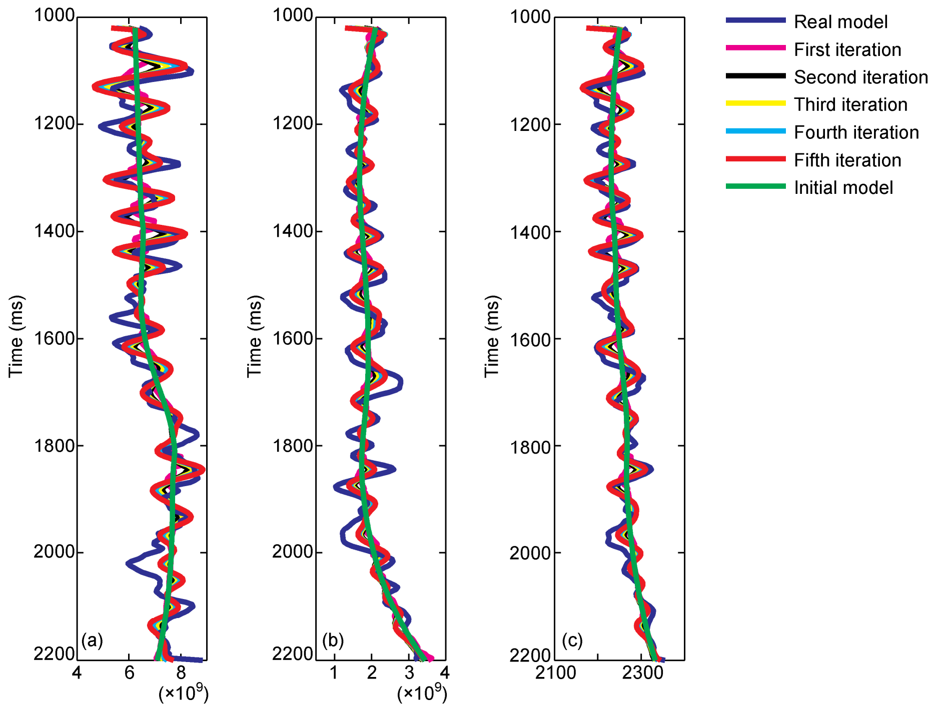

Figure 2 Model curves, initial models and the inversion results after five iterations without noise. (a) Fluid factor (N/m^2); (b) shear modulus (N/m^2); (c) density (kg/m^3).

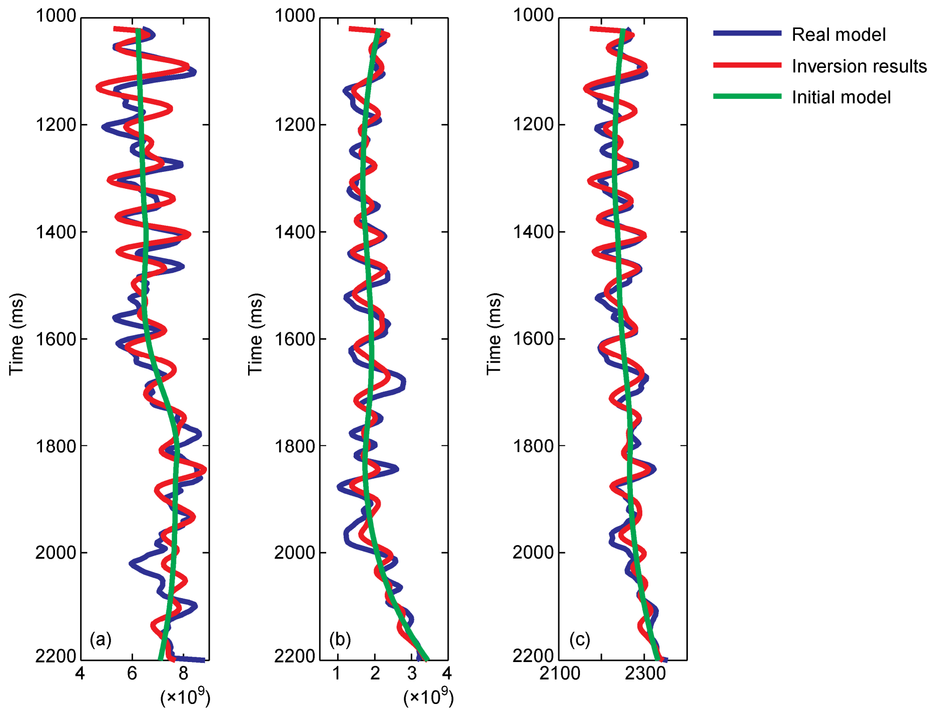

Figure 3 Model curves, initial models and the inversion results with S/N=5:1. (a) Fluid factor (N/m^2); (b) shear modulus (N/m^2); (c) density (kg/m^3).

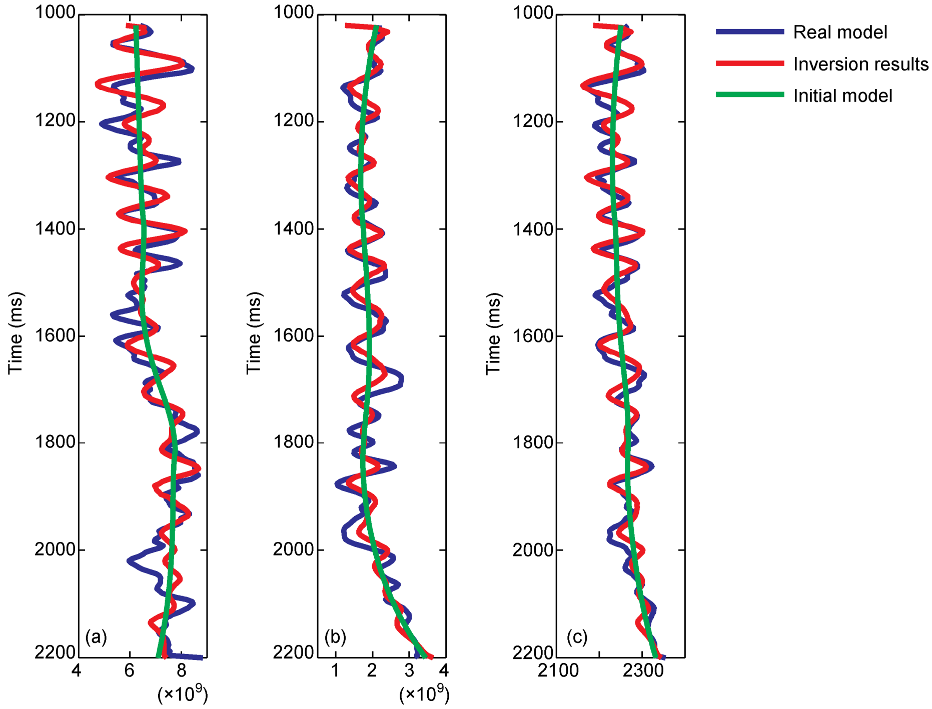

Figure 4 Model curves, initial models and the inversion results with S/N=2∶1. (a) Fluid factor (N/m^2); (b) shear modulus (N/m^2); (c) density (kg/m^3).

respectively. From the inversion result, we can see that the fluid factor, shear modulus and density still can be reasonably estimated with moderate noise, whose relative error is below 2%, which verifies the stability of this method.

4 Real data example

Before implementing seismic inversion, true-amplitude process should be performed including removal of multiples, corrections for the effects of geometrical spreading and absorption, inverse Q filtering. We assume that the mode conversions, interbed multiples, and anisotropy effects can be neglected after processing. After processing, the partial angle stack profiles through well A and B are shown in Figure 5, where the pink arrows denote the oil reservoirs, and the orange arrow denotes the oil-water reservoir. Figure 6 displays the initial smooth models of the fluid factor, shear modulus and density, respectively. Figure 7 displays the inverted results of the fluid factor, shear modulus and density with the proposed inversion method in this paper. From the inversion results, we can see that the fluid factor and density of reservoirs in well A and B decrease obviously, and the shear modulus in all four reservoirs has no obvious change, which is in line with the result of the analysis from well curves and drilling.

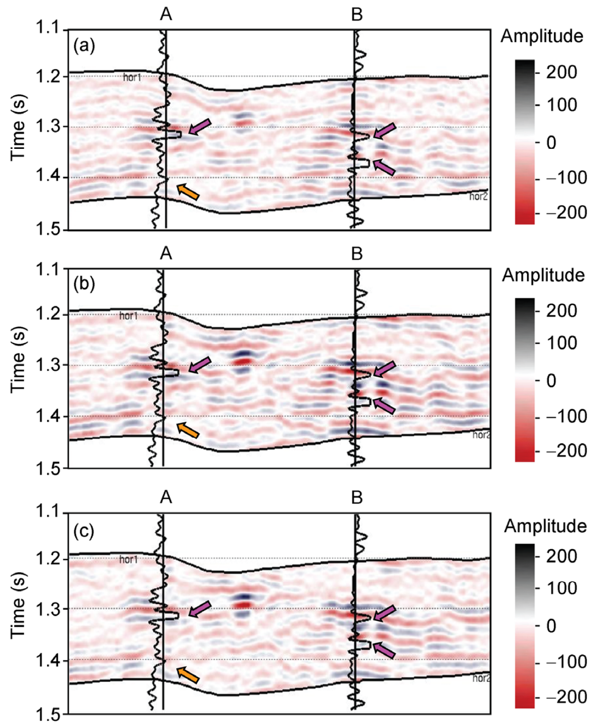

Figure 5 Partial angle stack seismic profiles. (a) Near angle; (b) middle angle; (c) far angle.

5 Conclusions

The description of heterogeneous reservoir, including lateral discontinuous, vertical overlapped sand reservoir, fracture-caved carbonate reservoirs and unconventional shale gas/oil reservoirs, has become one of the important research directions in oil/gas exploration. In this paper, an approach of fluid discrimination in heterogeneous media is proposed

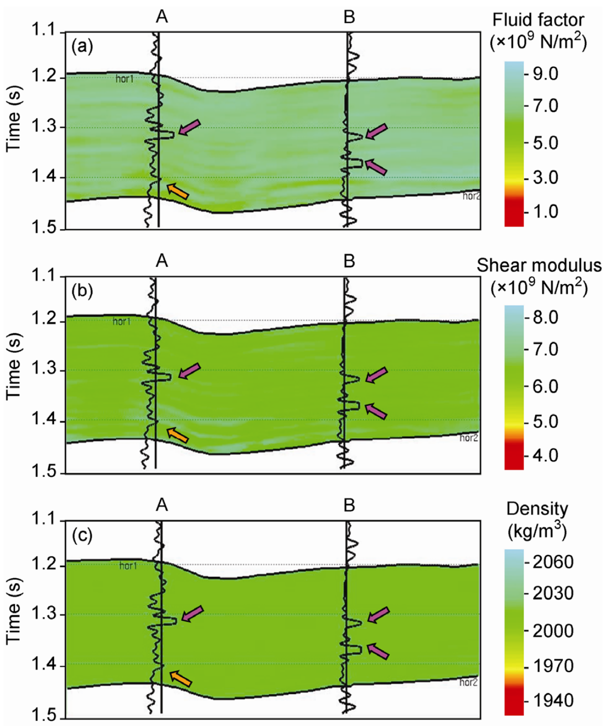

Figure 6 Initial models of parameters to be estimated. (a) Fluid factor; (b) shear modulus; (c) density.

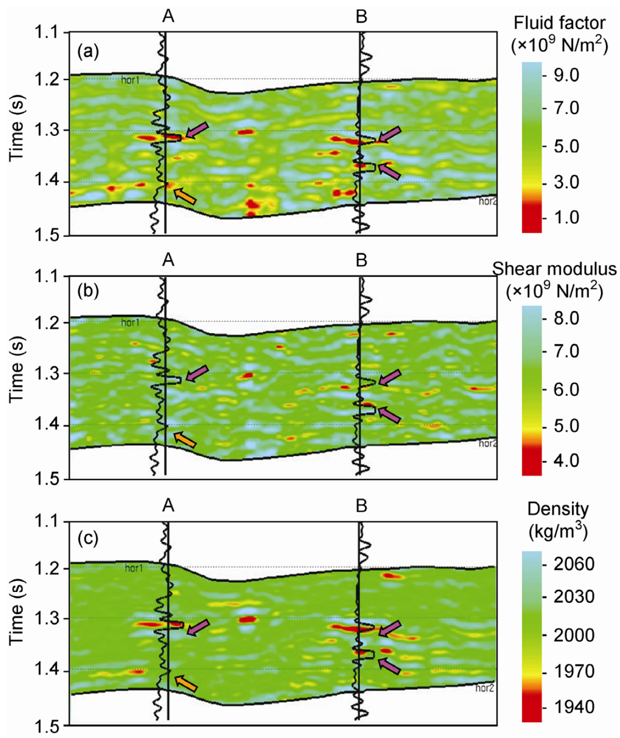

Figure 7 Inversion results with proposed inversion approach in this paper. (a) Fluid factor; (b) shear modulus; (c) density.

with the elastic wave inverse scattering theory, poroelsticity theory, and Bayesian inversion theory. With the stationary phase approximation, the seismic wave scattering efficient is derived in term of fluid factor, shear modulus, and density of the heterogeneous media. In the Bayesian inversion scheme, the introduction of the constraints from initial smooth model and multi-iterations enhances the stability of the proposed inversion approach. Model test shows that we can still obtain a reasonable inversion result with moderate noise in the observed data. Real data example demonstrates the feasibility of the proposed method in field production.

This study was supported by the National Basic Research Program of China (Grant No. 2013CB228604) and the National Grand Project for Science and Technology (Grant Nos. 2011ZX05030-004-002, 2011ZX05019-003 & 2011ZX05006-002). We acknowledge the support of the Australian and Western Australian Governments and the North West Shelf Joint Venture Partners as well as the Western Australian Energy Research Alliance (WA:ERA).

Beylkin G, Burridge R. 1990. Linearized inverse scattering problems in acoustics and elasticity. Wave Motion, 12: 15–52

Biot M. 1956. General solutions of the equations of elasticity and consolidation for a porous material. J Appl Mech, 23: 91–96

Biot M. 1962. Generalized theory of acoustic propagation in porous dissipative media. J Acoust Soc Am, 34: 1254–1264

Buland A, Omre H. 2003. Bayesian linearized AVO inversion. Geophysics, 68: 185–198

Burns D R, Willis M E, Toksoz M N, et al. 2007. Fracture properties from seismic scattering. Lead Edge, 26: 1186–1196

Cervený V. 2000. Seismic Ray Theory. Cambridge: Cambridge University Press. 124

Chen J J, Yin X Y. 2007. Three parameter AVO waveform inversion based on Bayesian theorem (in Chinese). Chin J Geophys, 50: 1251–1260

Downton J E, Lines L R. 2004. Three term AVO waveform inversion. Seg Tech Prog Exp Abs, 23: 215–218

Gassmann F. 1951. Uber die elastizitat poroser medien. Vierteljahrsschrift der Naturforschenden Gesellschaft in Zurich, 96: 1–23

Hudson J. 1968. The scattering of elastic waves by granular media. Q J Mech Appl Math, 21: 487–502

Hudson J. 1977. Scattered waves in the coda of P. J Geophys, 43: 8

Kaslilar A. 2007. Inverse scattering of surface waves: Imaging of near-surface heterogeneities. Geophys J Int, 171: 352–367

Liu F P, Meng X J, Wang Y M, et al. 2010. Jacobian matrix for the inversion of P- and S-wave velocities and its accurate computation method. Sci China Earth Sci, 54: 647–654

Liu E R, Chapman M, Zhang Z J, et al. 2006. Frequency-dependent anisotropy: Effects of multiple fracture sets on shear-wave polarizations. Wave Motion, 44: 44–57

Liu E R, Queen J H, Zhang Z J, et al. 2000. Simulation of multiple scattering of seismic waves by spatially distributed inclusions. Sci China E-Tech Sci, 43: 387–394

Liu E R, Zhang Z J. 2001. Numerical study of elastic wave scattering by cracks or inclusions using the boundary integral equation method. J Comput Acoust, 9: 1039–1054

Miles J W. 1960. Scattering of elastic waves by small inhomogeneities. Geophysics, 25: 642

Mora P, Sarwar A K M, Smith D L. 1987. Nonlinear two-dimensional elastic inversion of multioffset seismic data. Geophysics, 52: 1211–1228

Rajan S D, Frisk G V. 1989. A comparison between the Born and Rytov approximations for the inverse backscattering problem. Geophysics, 54: 864–871

Russell B H, Hedlin K, Hilterman F J, et al. 2003. Fluid-property discrimination with AVO: A Biot-Gassmann perspective. Geophysics, 68: 29

Scarpetta E, Tibullo V. 2008. On the oblique penetration of elastic waves into a finite number of equally spaced periodic arrays of obstacles. Wave Motion, 45: 518–539

Shaw R K, Sen M K. 2004. Born integral, stationary phase and linearized reflection coefficients in weak anisotropic media. Geophys J Int, 158: 225–238

Smith G C, Gidlow P M. 1987. Weighted stacking for rock property estimation and detection of gas. Geophys Prospect, 35: 993–1014

Stolt R H, Weglein A B, Abd Elhadi Y E. 1985. Migration and inversion of seismic data. Geophysics, 50: 2458–2472

Weglein A B. 1993. Nonlinear inverse scattering for multiple attenuation. Society of Photo-Optical Instrumentation Engineers Conference Series. 158–160

Wu R S, Aki K. 1985. Scattering characteristics of elastic waves by an elastic heterogeneity. Geophysics, 50: 582–595

Yang P J, Yin X Y. 2008. Nonlinear quadratic programming Bayesian prestack inversion (in Chinese). Chin J Geophys, 51: 1876–1882

Zhang H, Weglein A B. 2009a. Direct nonlinear inversion of 1D acoustic media using inverse scattering subseries. Geophysics, 74: 29–39

Zhang H, Weglein A B. 2009b. Direct nonlinear inversion of multiparameter 1D elastic media using the inverse scattering series. Geophysics, 74: 15–27

Zoeppritz K, Geiger L, 1919. Erdbebenwellen VIII B, Uber Reflexion and durchgang seismischer wellen duch unstetigkeitsflachen. Gottinger Nachr, 1: 66–84

Zong Z Y, Yin X Y, Wu G C. 2012a. Elastic impedance variation with angle inversion for elastic parameters. J Geophys Eng, 9: 24

Zong Z Y, Yin X Y, Wu G C. 2012b. AVO inversion and poroelasticity with P- and S-wave moduli. Geophysics, 77: N29–N36